16. B. C. Larson, C. W. White, T. S. Noggle, J. F. Barhorst, and D. M. Mills, *Appl. Phys. Lett.* **42**, 282 (1983).

17. B. C. Larson and J. F. Barhorst, *J. Appl. Phys.* **51**, 3181 (1980).

18. R. H. Lehmberg and S. P. Obenschain, *Opt. Commun.* **46**, 27 (1983).

19. D. Strickland and G. Mourou, *Opt. Commun.* **56**, 219 (1985).

20. P. Maine, D. Strickland, and G. Mourou (private communication).

2.B Thermal Conductivity in Dielectric Thin Films

In 1984 Decker *et al.*[1] reported the measurement of thermal conductivity for freestanding thin films of SiO_2 and Al_2O_3. Values were found to be one to two orders of magnitude lower than those for the corresponding bulk materials. The authors attributed this difference to the unique microstructure of dielectric thin films (primarily columnar for vapor-deposited coatings[2]), which, along with defects and impurities, would be expected to reduce the phonon mean-free path, and thus the conductivity. Work by others has recently reinforced these findings for other dielectric coatings.[3,4]

Low thermal conductivity has important implications for electronic and optical applications, where heat deposited in a thin dielectric layer must be dissipated to prevent damage. Models that account for thermal transport in multilayer thin-film structures[5] may have no predictive value if they employ bulk conductivity data.

Most techniques used to measure the thermal conductivity of dielectric materials in thin-film form are difficult and time consuming. This article describes a method developed at LLE[6] that is relatively rapid, nondestructive, and capable of evaluating samples in a conventional film-on-substrate geometry. The technique has the additional advantage of being able to study the thermal barriers created at interfaces between the coating and the substrate. We show preliminary data that suggest thermal conductivity varies considerably among dielectric coating materials.

Our thermal conductivity apparatus is shown schematically in Fig. 29.17. It consists of an environmentally isolated sample chamber, a control and readout module, and a data processor. The sample stage and control module were purchased in 1975[7] to perform conductivity measurements on bulk materials. The thermal comparator technique for determining bulk thermal conductivity has been extensively described by R. W. Powell.[8,9] The commercial unit was converted into a high-precision device by controlling the temperature of both the samples and sample stage, and by averaging the signal of the output data.

The principle of operation and the calibration procedure for the apparatus are shown in Fig. 29.18. After placing a test sample on the

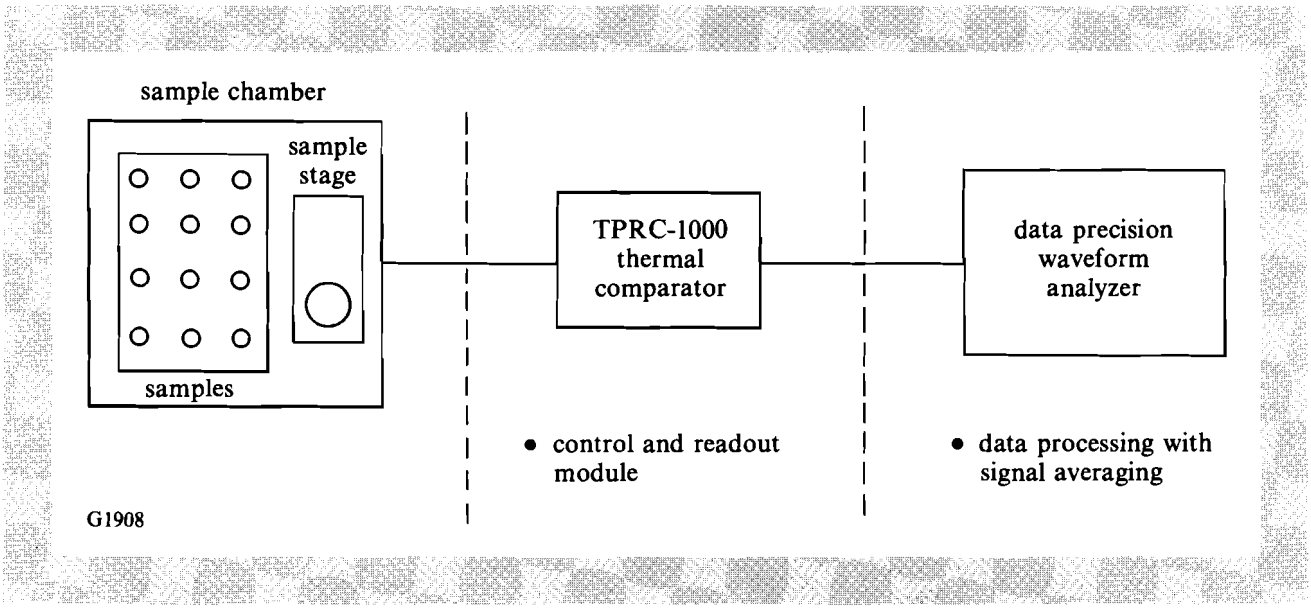

Fig. 29.17
High-precision thermal comparator apparatus. Samples and sample stage are contained in a sealed environmental chamber in which temperature is controlled to $\pm 0.1°C$, and humidity is kept constant at 6% $\pm 1\%$. A data precision waveform analyzer is used to acquire millivolt signals from the comparator readout module. The thermal comparator apparatus has been substantially modified from the commercial unit purchased in 1975.

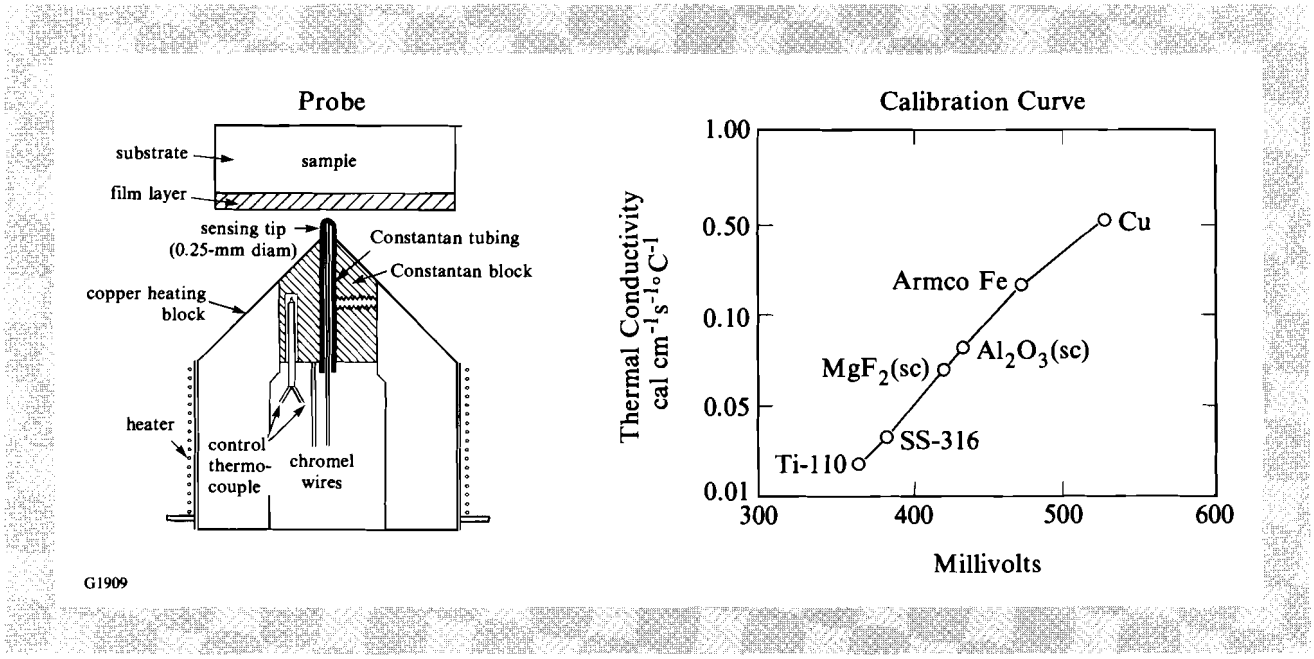

Fig. 29.18
Principle of operation. The tip of the heated thermocouple probe (56°C) is cooled when contacted to the coated substrate (36°C). A voltage generated between the probe junction and an internal, heated control junction reaches a steady-state value and is recorded. Thermal conductivity is determined by comparing calibration standard signals with unknowns. The thin-film coating causes a reduction in the conductivity of the substrate material.

sample stage, a thermocouple junction sensing tip is raised into contact with the sample surface. Heat flows from the hot tip (56°C to 66°C) to the cooler sample (36°C), and in approximately 10 seconds a steady-state condition is established. A voltage, generated by the temperature difference between the sensing tip and a reference junction, is acquired by the control module and displayed as a function of time on a waveform analyzer. Bulk solids of known conductivity are used to generate a thermal conductivity calibration curve (see Fig. 29.18), and unknowns are compared to these standards.

A highly conductive material, such as single-crystal silicon, is an optimum substrate for studying the conductivity of dielectric thin films. When a coated-silicon part is evaluated, the lower conductivity of the thin-film layer causes the substrate to register a reduced value of apparent conductivity. Measurements on a suitable set of coated substrates, in conjunction with a simple theoretical interpretation, provide a means for calculating the thermal conductivity of the thin-film material.

The model and assumptions for this work are illustrated in Fig. 29.19. We assume the heat flow to be perpendicular to all interfaces [see Fig. 29.19(a)]. The heat flux $\dot{Q}$ per unit area A from the probe tip into the sample is assumed constant through the thin film, any barrier layer, and the substrate. It is given as

$$\frac{\dot{Q}}{A} = \frac{k_f \Delta T_f}{h_f} = \frac{k_b \Delta T_b}{h_b} = \frac{k_s \Delta T_s}{h_s} \quad , \tag{1}$$

where we define the total temperature drop as

$$\Delta T_{\text{net}} \equiv \Delta T_f + \Delta T_b + \Delta T_s \, .$$

The absolute thicknesses and thermal conductivities of the thin-film/barrier layer/substrate combination are identified in Fig. 29.19(b). The net thermal conductivity of the combination k_{net} is then given by the relationship

$$\frac{\dot{Q}}{A} \equiv \frac{k_{\text{net}} \, \Delta T_{\text{net}}}{h_f + h_b + h_s} \quad ; \tag{2}$$

k_{net} is the quantity measured in our experiment. The thicknesses h_f and h_b of the film and any barrier layer are much less than the thickness of the substrate. By normalizing all thicknesses and conductivities in terms of the substrate thickness h_s and conductivity k_s we can derive the following relationship:

$$\frac{1}{K_{\text{net}}} = \left(\frac{1}{K_f} - 1\right) H_f + \left(\frac{1}{K_b} - 1\right) H_b + 1 \quad , \tag{3}$$

where $$K_{\text{net}} = \frac{k_{\text{net}}}{k_s} \, , \; H_f = \frac{h_f}{h_s} \, , \text{ etc.}$$

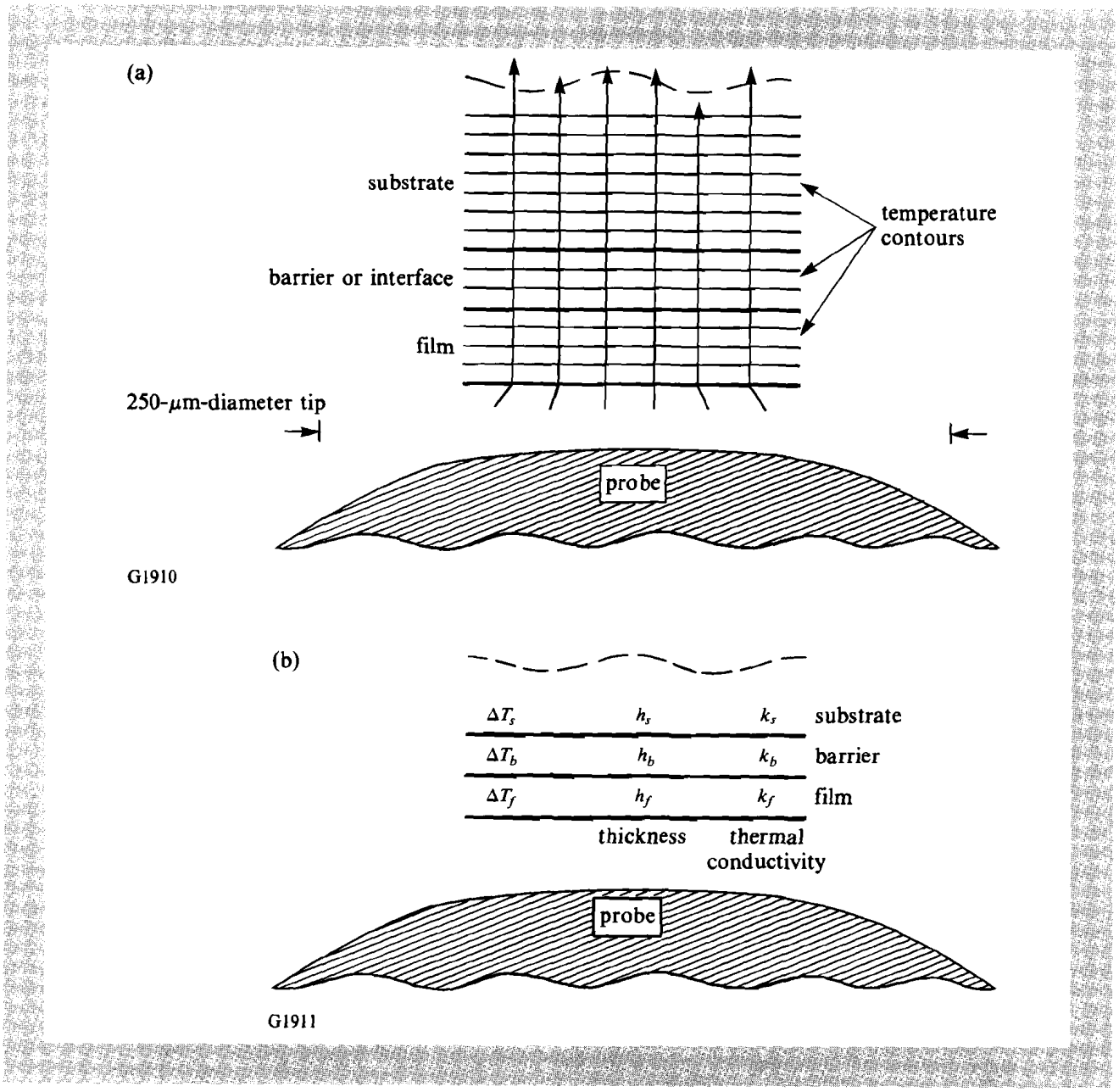

Fig. 29.19
Geometry and assumptions required to model experiment.
(a) The same heat flux $\dot{Q}$ is normal to the thin film, any barrier layer, and the substrate.
(b) The thicknesses and conductivities of the thin-film and barrier layers are normalized in terms of the substrate thickness and conductivity.

This is the equation for a straight line. By measuring the net conductivity k_{net} for a coating material deposited in different film thicknesses on a set of identical substrates, we can plot $1/K_{net}$ as a function of normalized film thickness H_f. The actual film conductivity k_f is derived from the slope of the straight line. The thermal conductivity of any barrier on interface layer k_b can be estimated from the zero thickness intercept of the line, providing reasonable assumptions concerning the barrier layer thickness h_b are made.

For experimental validation of our theory and approach, we examined single films of SiO_2 and Al_2O_3, deposited on single-crystal silicon substrates with a (111) surface orientation. The substrates were disc shaped, with dimensions of 50-mm diameter by 5-mm thickness. Their surfaces were 80/50 scratch/dig, ten fringes flat, and used as received from the vendor.[10] The coating depositions were carried out in our thin-film coating facility in a chamber equipped for *e*-beam evaporation. Single rotation was employed, substrate temperature was held at 200°C, and the O_2 partial pressure was 3×10^{-5} Torr during deposition. Materials were evaporated at a rate of 10 Å/s. We chose to deposit four film thicknesses per evaporant using an incremental coat/remove technique. This meant that the chamber was vented to air to remove one part each time a desired thickness was achieved. Coating thicknesses were estimated to be 0.5, 1.0, 2.0, and 4.0 μm $\pm 10\%$, based upon the output of an optical thickness monitor.

The photograph in Fig. 29.20 shows the location of test samples within the controlled environment chamber, and the method employed for sample placement during a set of measurement runs. The experiment is performed with samples at a temperature of 36°C to minimize thermal gradients introduced by the operator. Once mounted on the sample stage, a part is loaded with a 0.5-kg weight to prevent lifting from the contact pressure of the probe tip. During a set of runs, up to ten parts, consisting of coating and calibration samples, are sequentially measured. The measurement sequence is repeated several times over one to two hours to allow for a calculation of net thermal conductivity with an error estimate representing the reproducibility of the measurement.

G1912

Fig. 29.20
Instrumentation for thermal conductivity studies. Measurements are performed with the enclosure temperature at 36°C to minimize operator-induced temperature fluctuations. Samples are mounted on the sample stage and loaded with a 0.5-kg weight to insure uniform contact pressure with the probe tip. A run is completed in one to two hours.

The data for single films of SiO_2 and Al_2O_3 on silicon are shown in Fig. 29.21, where the reciprocal of normalized net thermal conductivity ($1/K_{net}$) has been plotted as a function of normalized film-layer thickness. From the slopes we calculate the thermal conductivities of the two materials to be as follows:

$$SiO_2\text{: } k_f = 4 \times 10^{-5} \text{ cal cm}^{-1}\text{s}^{-1}\text{°C}^{-1}$$
$$Al_2O_3\text{: } k_f = 5 \times 10^{-5} \text{ cal cm}^{-1}\text{s}^{-1}\text{°C}^{-1} \quad , \qquad (4)$$

with standard deviation, $\sigma = 1 \times 10^{-5}$.

The two values are the same within the standard deviation of the measurement. Because the zero thickness intercept is not equal to 1, we can make the observation that some form of low-conductivity barrier layer exists between the SiO_2 or Al_2O_3 coatings and the Si substrate. This barrier layer may be related to the oxidation of the Si substrate, and, if we assume it to be of the order of 10 Å to 100 Å in thickness, then a simple calculation suggests that the conductivity of the barrier layer is in the range of $\sim 10^{-7}$ cal cm^{-1}sec^{-1}°C^{-1}.

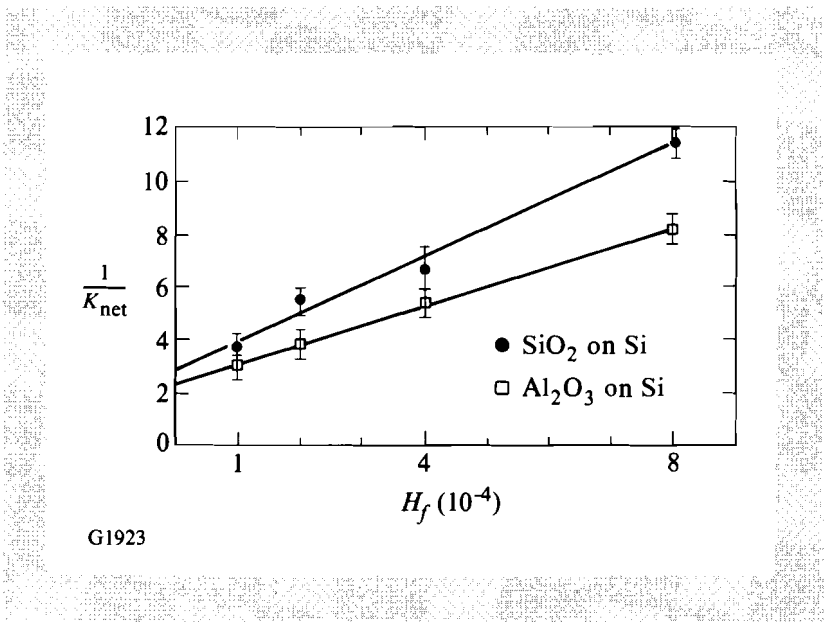

Fig. 29.21
Data for single films of SiO_2 and Al_2O_3 on silicon substrates. The reciprocal normalized net conductivity is plotted against normalized film thickness. Film conductivity is calculated from the slope of each line, and the effects of any barrier layers are related to the zero thickness intercept. Low conductivity is indicated (see text for details).

In a second experiment we examined single films of MgF_2 deposited on silicon, sapphire, and magnesium fluoride substrates. A description of the substrates is given in Table 29.II. The objectives of this experiment were to evaluate a fluoride film and to study substrate dependence.

The fluoride films were deposited under the same conditions as described above, except that the chamber was kept at its base pressure in the 10^{-6} Torr range. In addition, three separate coating runs were made to deposit each of three different film thicknesses on appropriate sets of substrates. The resulting thicknesses were measured with a Talystep surface profilometer and were found to be 0.6, 1.7, and 3.8 μm $\pm 5\%$.

Table 29.II
Substrate for MgF_2 single films

- Si
  - single crystal (111)
  - 45-mm diameter × 6-mm thickness
  - Polishing Corporation of America
- Al_2O_3
  - single crystal (*c*-axis 60° to face)
  - 25-mm diameter × 6-mm thickness
  - General Ruby and Sapphire Corp.
- MgF_2
  - single crystal (*c*-axis ⊥ to face)
  - 50-mm diameter × 5-mm thickness
  - Optovac, Inc.

G1962

Net conductivity measurements for the MgF_2 coatings on silicon were not reproducible. Close examination of the coatings showed tensile-stress fracture in films of all three thicknesses, and significant delamination was noted for the two thicker films after several weeks. We could obtain no useful information for this sample set.

The data for MgF_2 films on sapphire and magnesium fluoride substrates are shown in Fig. 29.22. The probe tip temperature was increased to 66°C for these measurements, which improved reproducibility by a factor of 2 compared to previously described results. No substrate dependence is observed, and from the zero slope we conclude that the film conductivity is essentially equal to that of the

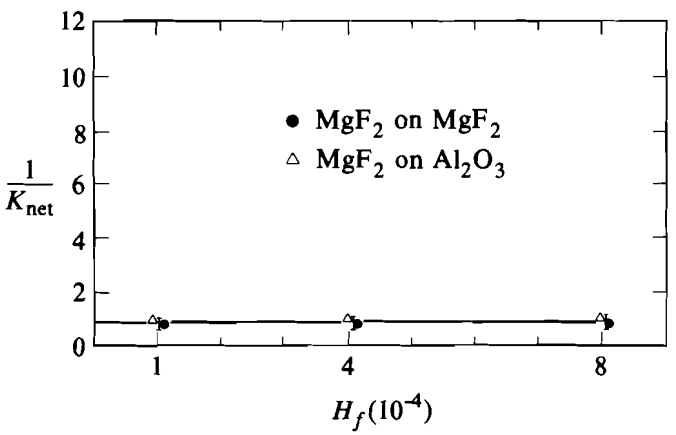

Fig. 29.22
Data for single films of MgF_2 on sapphire and magnesium fluoride substrates. The zero slope and unity intercept contrast sharply with the oxide film data in Fig. 29.21. High conductivity is indicated (see text for details).

substrates, which is 8×10^{-2} cal $cm^{-1}sec^{-1}°C^{-1}$. The microstructure of *e*-beam-deposited MgF_2 films is known to be polycrystalline,[11] whereas that of SiO_2 has been characterized as amorphous.[12] This may, in part, explain why the fluoride film conductivity compares favorably with the bulk and the oxide film data do not. The ordinate intercept at $1/K_{net} = 1$ indicates the absence of any barrier layer for these coating/substrate combinations, and this may be a result of the stability of sapphire and magnesium fluoride against oxidation.

Our results and those of two other groups[1,3] are compared on a logarithmic scale in Fig. 29.23. Values for single-crystal bulk solids Si, Al_2O_3, MgF_2, SiO_2, and fused silica are included for reference. We can make the following observations:

1. Oxide films exhibit thermal conductivities that are orders of magnitude below those of bulk solids.
2. One fluoride film, MgF_2, appears to exhibit a thermal conductivity representative of the bulk material.
3. A low-conductivity barrier layer exists for films deposited on single-crystal silicon, and it may be due to oxidation formed on the substrate surface prior to application of the oxide films.

In the future we will begin a thermal conductivity survey of dielectric coating materials, with special emphasis on ways to modify a given material's conductivity through the method of deposition. We will also extend the theory and experiment to multilayer structures.

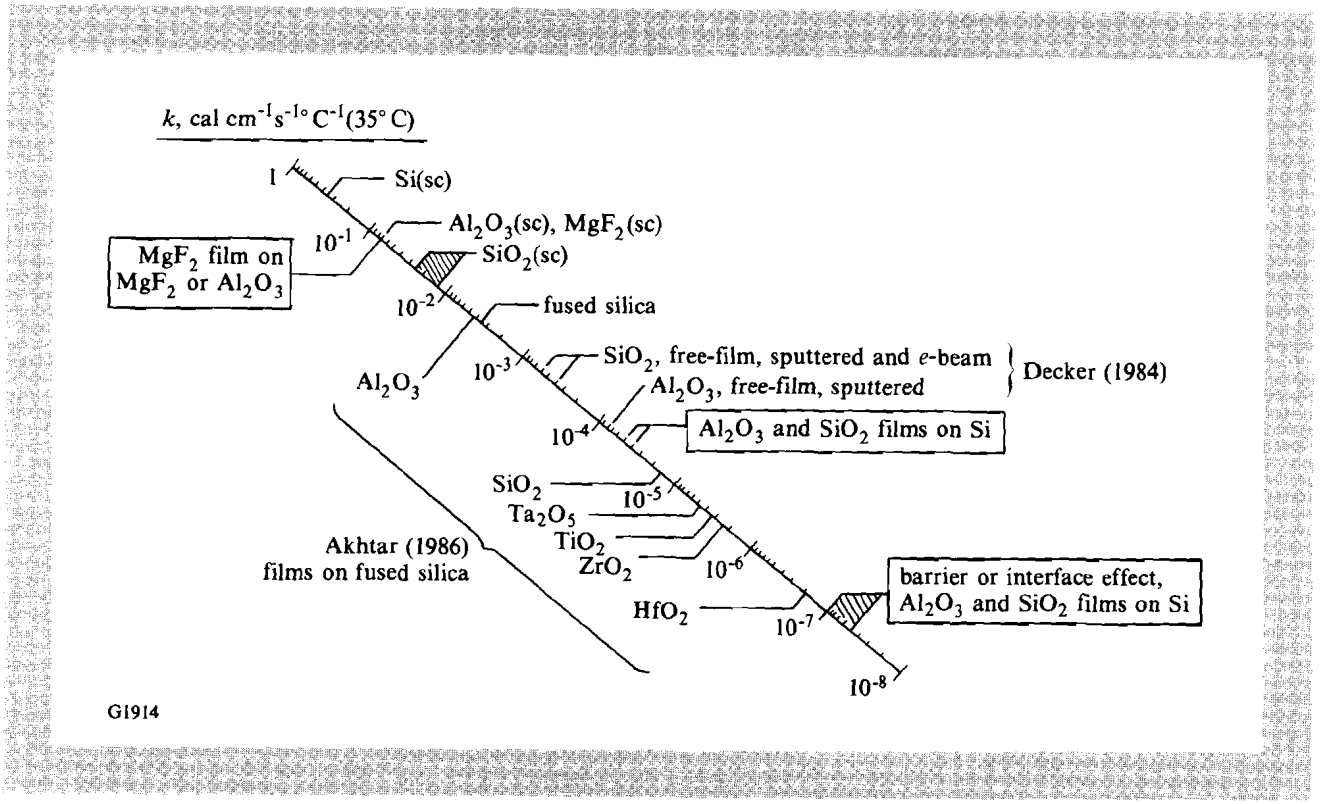

Fig. 29.23
Comparison of dielectric thin-film thermal conductivity results. Decker[1] *et al.* results are for freestanding oxide films; Akhtar[3] *et al.* results are for 1-μm-thick oxide films on fused-silica substrates.

ACKNOWLEDGMENT

This work was supported by the New York State Center for Advanced Optical Technology of The Institute of Optics, the U.S. Department of Energy Office of Inertial Fusion under agreement No. DE-FC08-85DP40200, and by the Laser Fusion Feasibility Project at the Laboratory for Laser Energetics, which has the following sponsors: Empire State Electric Energy Research Corporation, General Electric Company, New York State Energy Research and Development Authority, Ontario Hydro, and the University of Rochester. Such support does not imply endorsement of the content by any of the above parties.

REFERENCES

1. D. L. Decker, L. G. Koshigoe, and E. J. Ashley, *Nat. Bur. Stand. (U.S.), Spec. Publ.* **727**, 291–297 (1986).
2. See, for example, LLE Review **26**, 88–97 (1986); B. W. Krakauer, J. S. Gau, and D. J. Smith, *J. Mater. Sci. Lett.* **5**, 667–670 (1986).
3. S. M. J. Akhtar and D. Ristau, "Thermal Conductivity of Dielectric Films and Correlation to Damage Threshold at 1064 nm," presented at the 18th Annual Symposium on Optical Materials for High Power Lasers, Boulder, CO, 3–5 November 1986.
4. R. T. Swimm, "Photothermal Measurements of Optical Coating Thermal Transport Properties," presented at the 18th Annual Symposium on Optical Materials for High Power Lasers, Boulder, CO, 3–5 November 1986.
5. M. R. Lange, J. K. McIver, and A. H. Guenther, *Thin Solid Films* **125**, 143–155 (1985).
6. S. D. Jacobs, S. E. Gilman, D. G. Angeley, D. J. Smith, and J. C. Lambropoulos, "Thermal Conductivity in Dielectric Thin Films," presented at the Optical Society of America Annual Meeting, Seattle, WA, 20–24 October 1986.
7. TC-1000 Thermal Comparator, Lafayette Instrument Company, Lafayette, IN (no longer commercially available).
8. R. W. Powell, *J. Sci. Instrum.* **34**, 485–492 (1957).
9. R. W. Powell, in *Thermal Conductivity*, edited by R. P. Tye (Academic Press, London and New York, 1969), Vol. 2, Chap. 6, pp. 275–338.
10. Polishing Corporation of America, Santa Clara, CA.
11. H. K. Pulker and J. Maser, *Thin Solid Films* **59**, 65–76 (1979).
12. K. H. Guenther, *Appl. Opt.* **23**, 3806–3816 (1984).